

The Temporal Changes in Ankle Joint Pathology, Pain and Secondary Osteoporosis in Collagen-Induced Arthritis Rats

Qi Liu^{1,2,*}, Nan Nan^{1,2,*}, Wenfang Li^{1,2}, Mengwei Dong^{1,2}, Wei Pu^{1,2}, Yang Liu^{1,2}, Jie Zhao³, Huiqin Hao^{1,2}

¹Basic Laboratory of Integrated Traditional Chinese and Western Medicine, Shanxi University of Chinese Medicine, Jinzhong, 030619, People's Republic of China; ²Engineering Research Center of Cross Innovation for Chinese Traditional Medicine of Shanxi Province, Jinzhong, 03619, People's Republic of China; ³Shanxi Provincial Key Laboratory of Classical Prescription Strengthening Yang, Taiyuan, 030013, People's Republic of China

*These authors contributed equally to this work

Correspondence: Huiqin Hao, Email hhq@sxtcm.edu.cn

Background: Rheumatoid arthritis (RA) is a synovial inflammation-associated autoimmune disease with secondary osteoporosis. Pain is the most important symptom of RA, and some patients with well-controlled inflammation may still experience pain.

Purpose: To explore the relationship and dynamic changes between synovial inflammation and pain and bone destruction in collagen-induced arthritis (CIA) model rats, and to choose a better time window for drug treatment.

Methods: The CIA model rats were constructed for 1, 2, 3, and 4-week groups. The changes were observed by joint swelling and behavioral assessment. The paw mechanical withdrawal threshold (PWT) was used for pain assessment. The micro-CT was used to assess joint injury and bone destruction. The biomechanics were performed to evaluate tension and compression test. The histological staining was used to observe ankle joint pathology. The immunohistochemical staining and Western blot were used to estimate the expression of calcitonin gene-related peptide (CGRP) and c-fos.

Results: The results showed that the degree of joint swelling, synovial hyperplasia, and inflammatory response were alleviated to varying extents over time. However, there were no significant changes in bone destruction, osteoclasts, or the maximum load of compression and tension. It showed secondary osteoporosis from the first week of the CIA model with no significant changes during the course of the experiment. There was no significant improvement in the PWT, and the expression of CGRP and c-fos was significantly increased over time, indicating hyperalgesia aggravation. Additionally, the result showed that repeated open-field tests might reduce the total distance of spontaneous movement.

Conclusion: The results suggested that the pain and joint inflammation might not be synchronized, possibly related to post-inflammatory hyperalgesia. CIA model could be used for the study of pain, also relatively stable and suitable for the study of RA with secondary osteoporosis.

Keywords: collagen-induced arthritis rats, temporal changes, inflammation, pain, secondary osteoporosis

Introduction

Rheumatoid arthritis (RA) is an autoimmune disease with redness, swelling, heat, and pain as the main clinical manifestation of joints. The mechanism of RA is joint synovial inflammation, which eventually leads to cartilage destruction, bone damage, joint dysfunction, and deformity. RA affects approximately 1% of the global population and leads to significantly increased disability and economic burden.

Pain is one of the biggest and most priority issues in RA patients.¹ It is attributed to peripheral inflammation in the affected joints. Currently, non-steroid anti-inflammatory drugs, biological or non-biological antirheumatic drugs can partially relieve the symptoms of inflammatory pain. However, there remains still moderate pain in many patients, with confirmed pain of central sensitization association in 41% of RA patients in a clinical study.² In the early stages of RA, pain sensation is

dominated by the release of pro-inflammatory cytokines localized in the joint. With the development and treatment of RA, persistent afferent pain activates multiple pain pathways,³ causing synaptic changes and dysregulation of the central nervous system pain circuit, eventually leading to the impairment of central pain regulation mechanisms. Current models used in research of RA include collagen-induced arthritis (CIA), adjuvant-induced arthritis type (AIA),⁴ collagen antibody-induced arthritis type (CAIA),⁵ K/BxN serum-transfer arthritis (STA)⁶ and so on. The latter three models all showed symptoms of pain after the inflammation subsided, which suggested some correlation and independence between synovial inflammation and joint pain. It suggested that there might be a state of post-inflammatory hyperalgesia.^{7,8} Several studies have found that the ankle redness and swelling of CIA rats had different degrees of relief with the extension of the molding time,^{9,10} but the trend in its pain is unclear. In addition, synovial inflammation could also lead to bone mass decrease, bone tissue microstructure damage, bone fragility increase, and fracture risk increase, eventually promoting the emergence of secondary osteoporosis (OP). The researchers found that the overall incidence of OP in RA patients was twice that of normal individuals,^{11,12} and the incidence of brittle fractures in RA patients significantly increased (relative risk:1.61).¹³ The CIA model rats showed decreased bone density and destruction of bone trabecular structure.¹⁴ It is consistent with the pathological characteristics of RA combined with secondary OP, but the process of bone destruction in this model is still unclear.

At present, the clinical treatment of RA mainly focuses on inflammatory indicators and their related joint pain and swelling. The attention to joint pain and OP after inflammation is often insufficient. Both pain and bone destruction are important indicators to evaluate the clinical efficacy of RA. The characteristics of pathological changes at different stages determine the choice of treatment methods and strategies and help to predict the disease process and improve the recovery effect of patients. Therefore, this study established the CIA model rats to observe the ankle joint pathology, pain threshold and secondary osteoporosis changes of the paw joint and also investigated whether there is consistency between inflammation and them, to provide ideas for selecting models and determining the treatment time window when researching RA joint pain and OP.

Materials and Methods

Establishment and Grouping of the CIA Model Rats

Thirty-five Sprague-Dawley (SD) rats (aged 7–8 weeks, weighing 200 ± 20 g) were purchased from BEIJING HFK BIOSCIENCE Co., LTD. and housed in the Laboratory Animal Center of Shanxi University of Traditional Chinese Medicine with a temperature between 22 and 24°C, humidity between 55%–60%, and light/dark cycle for 12h. All the rats could get food and water freely. The protocols of this test were approved by the Experimental Animal Ethics Committee of Shanxi University of Traditional Chinese Medicine (AWE202302161). Six rats were randomly selected as the control group (Control). On Day 1, the tail root of other twenty-nine SD rats were injected subcutaneously with 1mg/mL complete Freund's adjuvant (7001, Chondrex, USA) emulsified with type II collagen (20022, Chondrex, USA) at a ratio of 1:1, and incomplete Freund's adjuvant (7002, Chondrex, USA) and type II collagen on Day 14.¹⁵ On Day 21, twenty-four rats with an arthritis index ≥ 4 were regarded as CIA models which were divided into 4 groups (1w, 2w, 3w, 4w) ($n = 6$). To observe the degree of joint for 4 weeks and the change of pathological every week. The hind paws were fixed with 4% paraformaldehyde buffer (pH 7.4) for CT and slices. The L4-6 spinal cords were stored in 4% paraformaldehyde buffer and -80°C for immunofluorescence staining and WB. The femoral were collected in gauze moistened with saline and stored at -80°C .

Ethology

The body weight, arthritis score, and paw swelling were measured weekly.¹⁶ Von-Frey filament (NC12775-99, YunYan instrument, China) was used to detect the changes in the mechanical withdrawal threshold in the left hind paw as described in reference.¹⁷ The filaments of 1g–26g were used to stimulate until the rats contracted or licked the paw or screamed and recorded the number of grams, which was the paw mechanical withdrawal threshold (PWT). The open field (OF) analysis system (XR-Xmaze, XinRuan Technology, China) was used to observe the total distance, rest time, and speed of control and 4w groups in 5 minutes.

Micro-CT

The micro-CT (IRIS PET/CT, Inviscan, France) was used to scan the left hind paw with a voltage of 80kv, current of 1mA, projection times of 2000, exposure time of 56ms, resolution of 60um. The scanning results were used for 3D image reconstruction. The calcaneus was selected as the region of interest (ROI) for the quantitative analysis of the bone microstructure, including the bone volume/tissue volume (BV/TV), bone mineral density (BMD), trabecular thickness (Tb.Th), trabecular separation (Tb.Sp).

Biomechanical of Femur

The femoral samples were placed slowly and thawed at room temperature before the test. The tension and compression tests were performed with an electronic universal tester (Byes1050, B-yes, China) for the biomechanical of femurs. The two ends of the femur were fixed on the tester, and the speed of the tester was set to 1mm/min until the sample failed completely. Avoid bone rotation and lateral displacement during the tests and the maximum load was recorded for analysis.

Elisa

The blood was collected through the abdominal aorta, and serum was obtained after centrifuging 20 min at 3000 rpm/min and 4 °C. The levels of serum cytokines IL-1 β (MM-0047R2, MEIMIAN, China) and TNF- α (MM-0180R2, MEIMIAN, China) in each group of rats were measured by ELISA kit according to the instructions.

HE and TRAP Staining

After the right hind paw was fixed in paraformaldehyde for 48h and decalcified in 0.5M EDTA with pH 7.2 (G1105, Servicebio, China). The ankles were embedded, and sectioned. The paraffin sections were dewaxed and washed in pure water. Hematoxylin and eosin for HE staining were used to observe the synovial hyperplasia and inflammatory infiltration of the ankle joint. Meanwhile, the sections were incubated in TRAP staining solution (G1050, Servicebio, China) as described in the reagent instructions.

Western Blotting

Briefly, the tissues of the spinal cord were homogenized and centrifuged. The protein concentrations of supernatants were determined by a bicinchoninic acid kit (AR0146, BOSTER, China). Proteins were separated in 10% gradient gels via sodium dodecyl sulfate-polyacrylamide gel electrophoresis and passed to a PVDF (polyvinylidene fluoride) membrane. The non-specific binding site on PVDF was blocked with 5% non-fat milk (T1081, Solarbio, China) for 2h, and the membranes were washed and placed in primary antibodies overnight at 4°C: anti-c-Fos (ab190289, 1:1000, Abcam, USA); anti-CGRP (AB139264, 1:1000, Abcam, USA) for TNC; anti-GAPDH (GB12002, 1:10000, Servicebio, China). The horseradish peroxidase-conjugated secondary antibodies (GB23301 and GB23303, 1:10000, Servicebio, China) were incubated with the membranes for 1h at room temperature. The antibody-reactive bands on the membrane were detected by an enhanced chemiluminescence reagents kit (AR1197, BOSTER, China) by an imaging system (ChemiDoc, BIO-RAD, USA) and analysis by Image J software.

Immunofluorescence Staining

The tissues of the spinal cord were embedded in paraffin and sectioned after postfixing. Place the tissue sections in 1 \times sodium citrate retrieval solution (pH = 6.0) and perform high-temperature and high-pressure for 2 minutes. The sections were incubated with anti-c-Fos antibody (1:500, Abcam) and secondary antibodies. The sections were then incubated with DAPI for 10 min. The fluorescence was obtained by a panoramic scanner.

Statistical Analysis

Statistical analyses and graph generation were performed with GraphPad Prism 8 (GraphPad Software, San Diego, CA). Two-way analysis of variance (ANOVA) with a Holm-Sidak's multiple comparisons test was used for weight, arteries score, paw swelling, PWT and OF test, with model and time as factors. One-way ANOVA followed by Bonferroni's post

hoc test was used to analyze the other results. If the data were not normally distributed, the Kruskal–Wallis test followed by Dunn's test was used. All data were shown as the mean \pm standard deviation (SD), and $p < 0.05$ indicated statistical significance.

Results

Temporal Change of Weight and Joint in CIA Rats

We followed the procedure of Figure 1A for experimental observation. The results showed that there are no significant differences in body weight, arthritis score, and paw swelling of rats in each model group after the CIA model achieved (0 week, Figure 1B–D). The weight of CIA rats significantly decreased ($P < 0.05$) compared to the control group at the same time point in, Figure 1E and arthritis score and paw swelling both significantly increased in Figure 1F and G ($P < 0.05$). With the extension of the modeling experiment, the arthritis score and paw swelling of rats in each model group showed varying degrees of recovery and more obvious performance in the 3w and 4w groups.

Temporal Change of Pain and Central Hyperalgesia in CIA Rats

The paw mechanical withdrawal thresholds of the model groups were lower than that of the correspondent control group ($P < 0.05$), and there was no significant difference among the model groups (Figure 2E). In the OF test, the total distance and average speed of model rats maintained a lower level compared with the control group at the beginning. While the

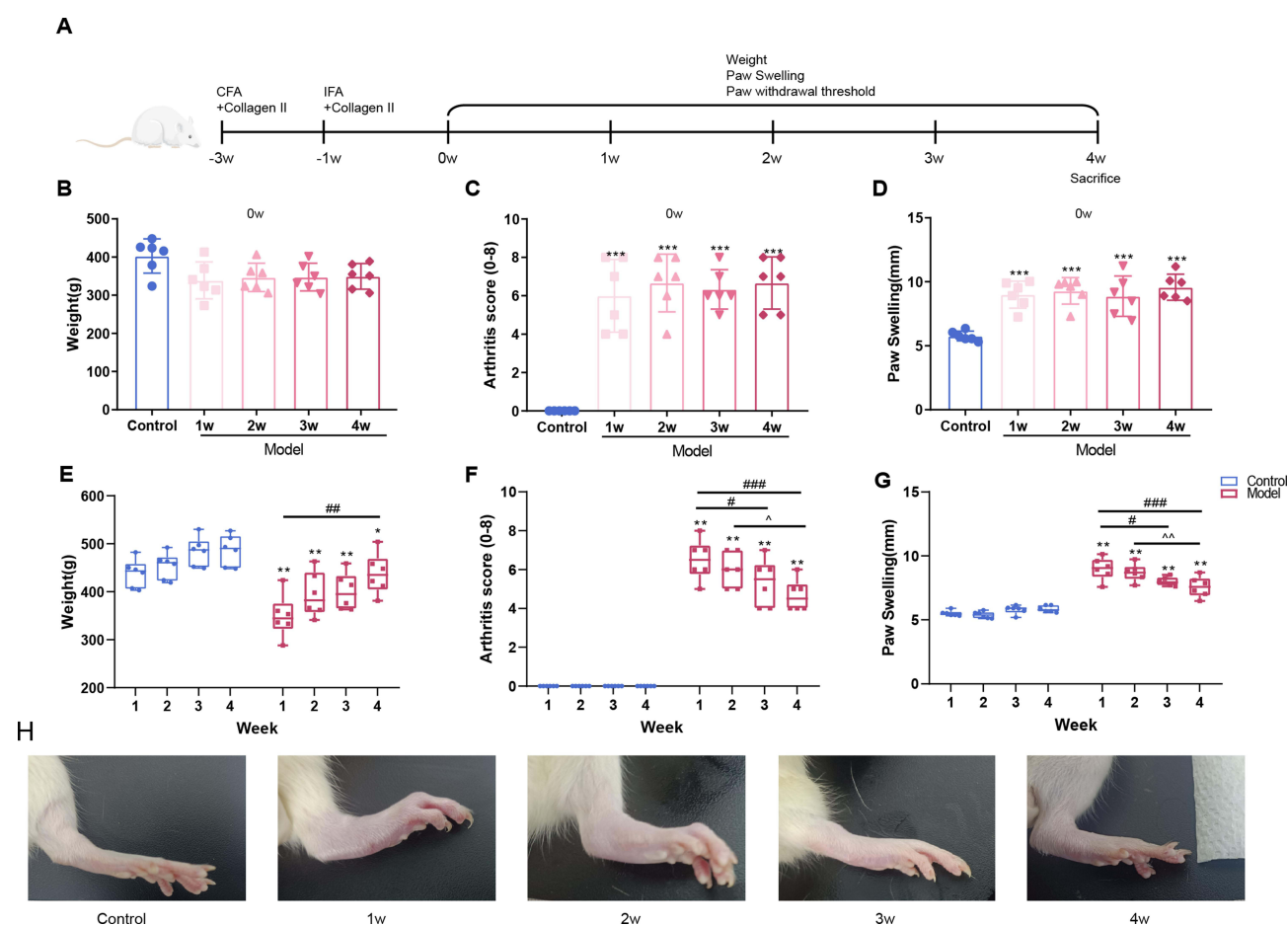


Figure 1 The temporal change of ankle joint in CIA rat. (A) The chart of experimental flow. The observation was initiated after the initial immunization 3 weeks (0w). (B–D) The body weight, arthritis score, and paw swelling of each group were measured at 0w. The CIA model showed arthritis score and paw swelling increased. $n=6$, One-way ANOVA analysis. (E–G) The body weight, arthritis score, and paw swelling of each group were measured. The weight of CIA rat increased, arthritis score and paw swelling decreased during 1–4 week. $n=6$, Two-way ANOVA analysis. (H) Representative image of the rat paw showed the redness and swelling. Compared to Control group, * $P < 0.05$, ** $P < 0.01$, *** $P < 0.001$. Compared to 1w group, # $P < 0.05$, ## $P < 0.01$, ### $P < 0.001$. Compared to 2w group, ^ $P < 0.05$, ^^ $P < 0.01$.

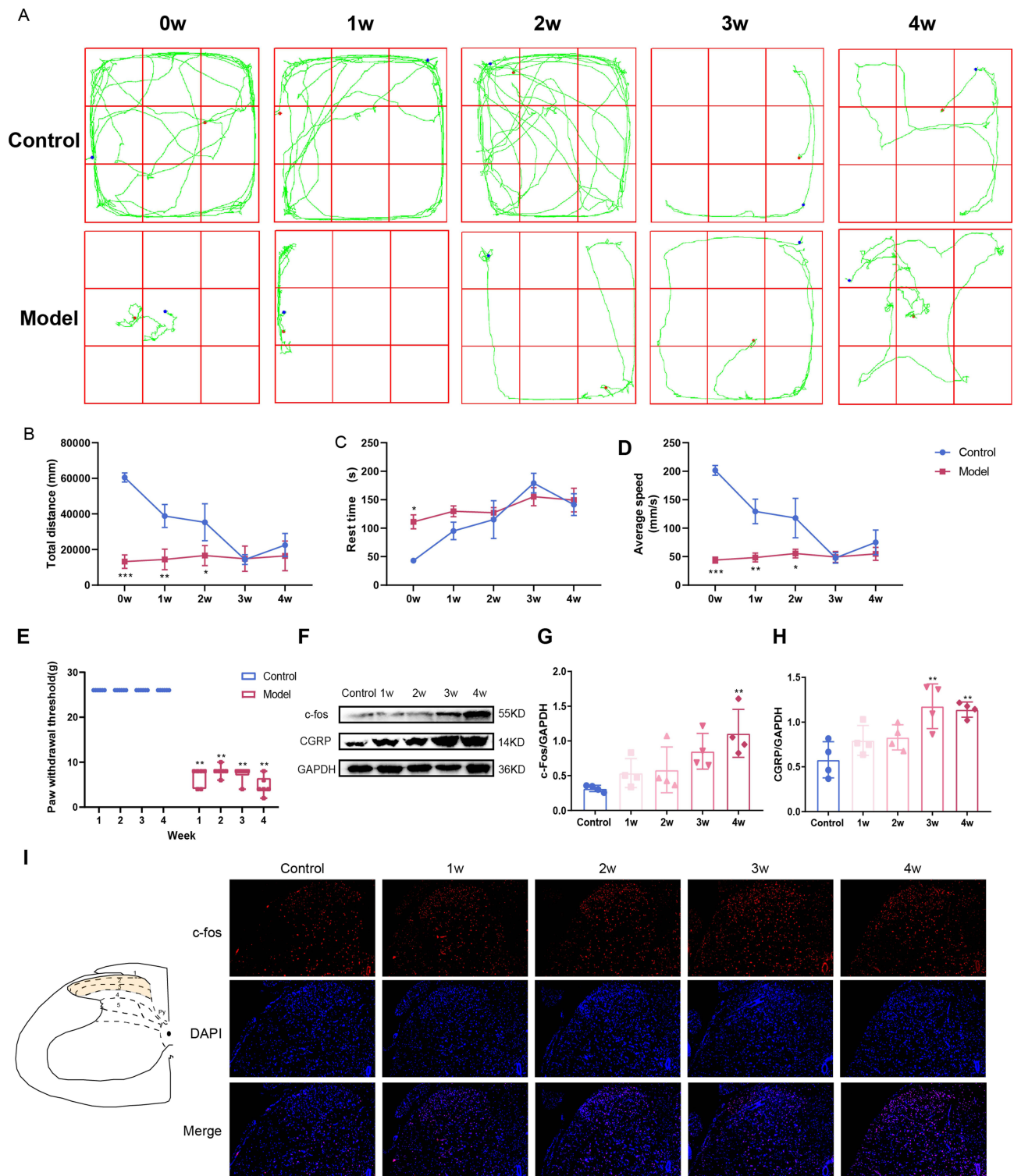


Figure 2 The temporal change of pain and central hyperalgesia in CIA rats. **(A–D)** The OF test were performed to assess the distance, rest time, and average speed of CIA rats. The CIA model rats exhibited reduced activity and the control rats exhibited a gradual decrease in movement distance. $n=6$, Two-way ANOVA analysis. **(E)** Paw withdrawal threshold was assessed using the von Frey test reflecting the degree of pain tolerance. $n=6$, Two-way ANOVA analysis. **(F–H)** The protein expression of c-fos and CGRP in spinal cord was tested by WB. $n=4$, One-way ANOVA analysis. **(I)** Representative image of spinal for c-fos detected by IF staining. The fluorescence intensity was gradually enhanced during 1–4 week. Compared to the Control group, * $P < 0.05$, ** $P < 0.01$, *** $P < 0.001$.

control group continued to decrease with the increase in the number of OF test, until there was no significant difference between the control group and the model group rats (Figure 2A–D). However, the results of protein expression showed significant increases in CGRP and c-fos in the spinal cord, and it also showed a certain time dependency with the course of the disease (Figure 2F–H). The c-fos-positive neurons in spinal dorsal horn regions related to pain processing showed (Figure 2I).

The Temporal Change of Inflammatory Response in CIA Rats

Compared with the control group, the levels of inflammatory factors IL-1 β ($P<0.05$) and TNF- α in the serum of model rats increased at 1w, and then the inflammatory factors gradually decreased. IL-1 β was significantly lower at 2w than at 1w ($P<0.05$) and showed no significant difference compared to the control group (Figure 3A and B). With the extension of modeling time, the HE staining results showed that the proliferation and inflammatory response of the joint synovium were reduced and the joint space increased to varying degrees (Figure 3C).

The Temporal Change of Bone Destruction in CIA Rats

The results showed that the joint surfaces of rats in all model groups were rough, and the joint structures were unclear with severe bone destruction (Figure 4A). The analysis of the calcaneal bone mass showed that BV/TV, BMD, AND Tb.Th in model rats were significantly reduced (Figure 4B–D), while Tb.Sp showed an increasing trend (Figure 4E). It is suggested that the CIA model rats have severe secondary OP, which is time-dependent and will not improve in a short period with the amelioration of inflammation. TRAP staining showed that the number of positive cells significantly increased in the ankle of all CIA model rats and there was little difference among the CIA model groups (Figure 4F).

The Temporal Change of Bone Biomechanics in CIA Rats

The results showed that the maximum load of femoral tension was significantly reduced in the model groups compared to the control group in Figure 5A ($P<0.05$). However, in the compression tests, the maximum load of femur compression in the model groups gradually increased as the disease progressed in Figure 5B ($P<0.05$), which does not completely correspond with the trend of bone destruction indicated by CT scans and the tension test.

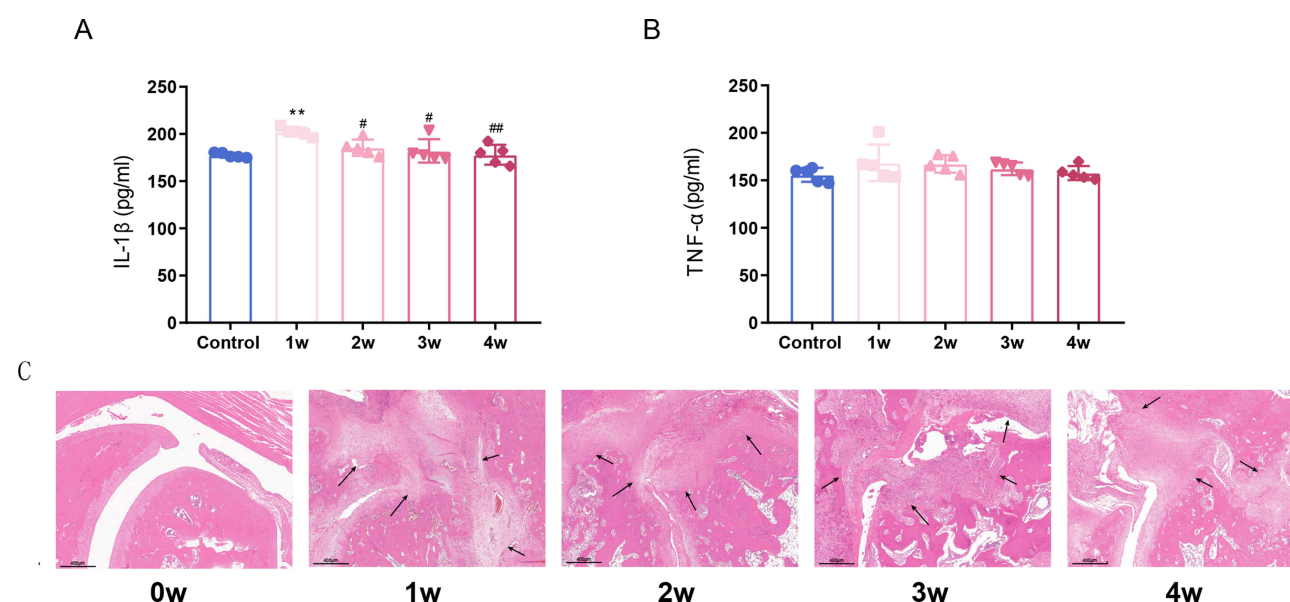


Figure 3 The temporal change of inflammatory response in CIA rats. [(A–B) The level of IL-1 β and TNF- α in serum detected by ELISA. The content of IL-1 β was increase at 1 week and then reduced during 2–4 week. $n=5$, One-way ANOVA analysis. (C) Representative pathological sections of the ankle joint using H&E staining. The inflammation of synovial were indicated with the black arrow. Compared to the Control group, ** $P<0.01$. Compared to 1w group, # $P<0.05$, ## $P<0.01$.

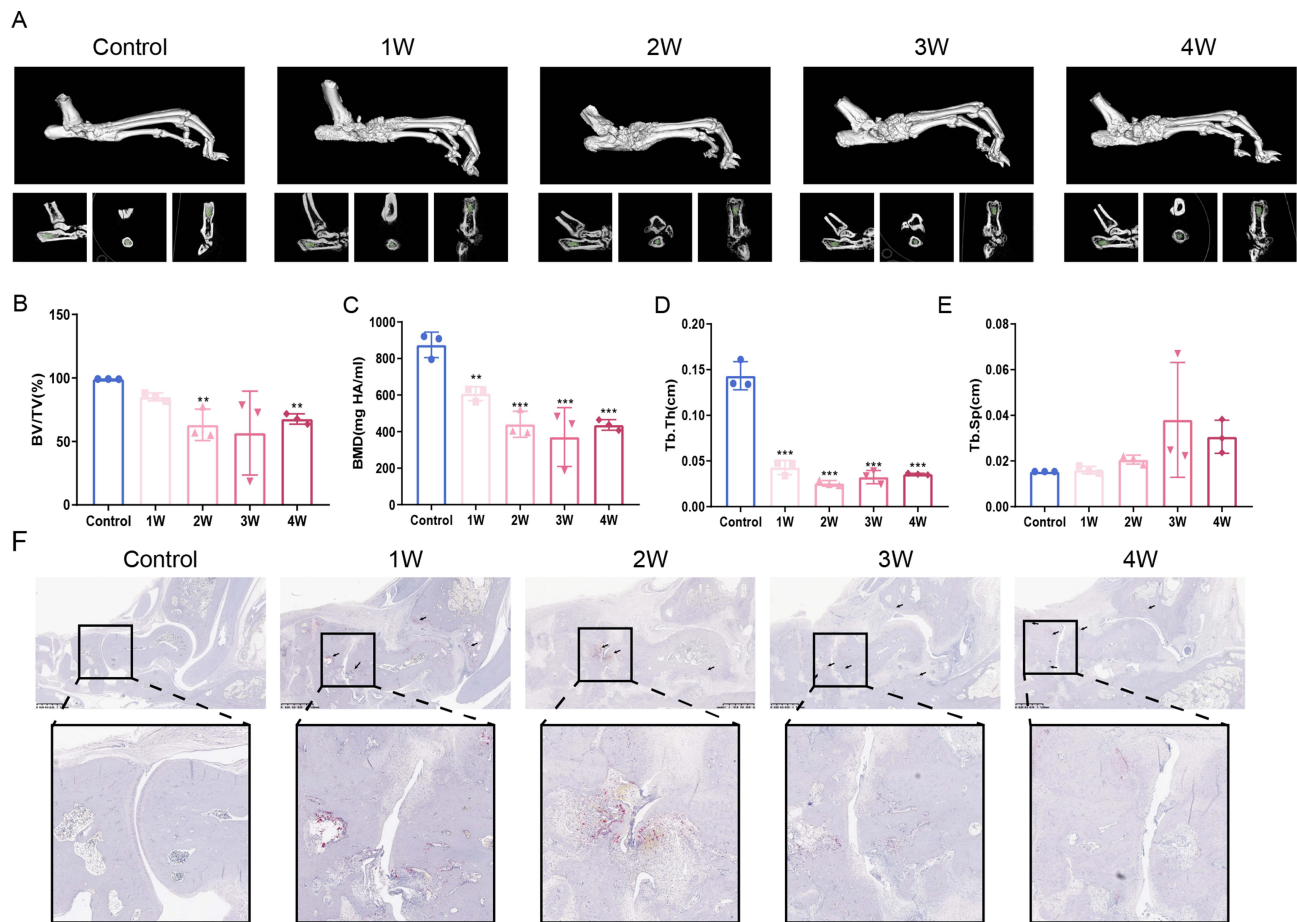


Figure 4 The temporal change of bone destruction in CIA rats. **(A)** Representative 3D reconstruction image of paws detected by micro-CT. The ROI region was selected in the calcaneus bone. **(B–E)** Bone volume fraction (BV/TV), bone mineral density (BMD), trabecular thickness (Tb.Th), and trabecular separation degree (Tb.Sp). $n=3$, One-way ANOVA analysis. Compared to the Control group, ** $P<0.01$, *** $P<0.001$. **(F)** Representative images of the ankle joint using TRAP staining. The osteoclasts were stained in wine red and indicated with the black arrow.

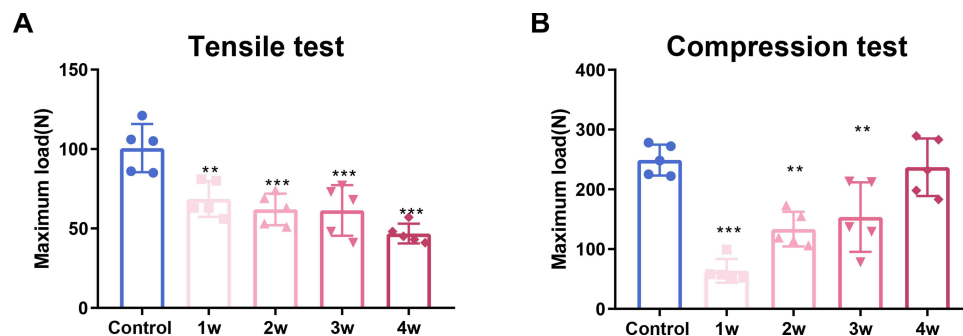


Figure 5 The temporal change of bone biomechanics in CIA rat. **(A)** The maximum tensile load of the femur was assessed by the electronic universal tester. **(B)** The maximum compression load of femur was assessed by the electronic universal tester. $n=5$, One-way ANOVA analysis. Compared to the Control group, ** $P<0.01$, *** $P<0.001$.

Discussion

The weight, joint swelling, ankle diameter, and paw diameter of CIA rats were gradually decreased 4 weeks after the first immunization. The content of serum inflammatory factor $\text{TNF-}\alpha$ and $\text{IL-1}\beta$ were also gradually decreased. The degree of synovial erosion in the joints was slightly reduced by HE staining. These results suggested that the joint inflammation of CIA model rats was reduced. However, the paw mechanical withdrawal threshold and the total distance of OF were not improved

with the reduction of inflammation, and the expression of CGRP and c-fos in the spinal cord increased with prolonged immunization. Interestingly, it was found that the total distance of the control rats gradually decreased in the OF test. It might be due to the rats forming a memory of OF test environment in repeated experiments, leading to reduced exploratory behavior and their activity area. This trend is similar to findings reported in related research.¹⁸ In addition, the CT results indicated that there was no significant improvement in ankle bone destruction among all the model group and there was no significant reduction in the number of osteoclasts shown by TRAP staining. Tensile tests used to assess the maximum load of femurs indicate that the severity of OP is progressively increasing. However, the maximum loads measured in compression tests are gradually increasing over time. It might be associated with the aggravation of osteoporosis. In addition to bone cancellous, the bone cortex of the femur also developed more severe osteoporosis. The bone mineral density of cortical and cancellous bone is relatively close. The microfractures were induced by smaller forces. The decreased probability of a longitudinal disintegration of the bone cortex. The load reduction caused by the compression of the bone structure failed to reach the preset value (20%) and record, with a compression effect similar to the solid material. Until the compressive force is large enough to cause severe fractures, this results in a significant reduction in the force exerted. Thus, the load decreased to the preset value and a higher recorded compressive load. This is the reason that the maximum Von Mises stress value of the best cortical reinforcement was significantly smaller than that of the non-cortical reinforcement. The Von Mises stress value showed a downward trend with extensive cortical reinforcement in the same plane.¹⁹ Therefore, this model also has a state of post-inflammatory hyperalgesia, and it can be used for the study of OP.

Chronic neuropathic pain refers to chronic pain caused by damage or disease of the bodily sensory nervous system, which exists in the absence of noxious stimuli and surrounding inflammation with an increased response to painful or non-painful stimuli.²⁰ The increasing evidence suggests that there might be neuropathic features of the pain experienced by many RA patients.²¹ Clinical studies have also found that the pain threshold of the tissue near the joint was reduced and more analgesic drugs were applied in the absence of persistent local inflammation or tissue damage. The widespread distribution of nociceptive sensitization suggests that persistent pain was caused by central pain regulatory mechanisms rather than peripheral stimulation of nociceptors.²² The pain can produce neuroendocrine responses and release neurotransmitters such as CGRP which maintains and strengthens hyperalgesia and glial responsiveness around the spinal cord.²³ The neuroendocrine responses could promote neurogenic inflammation and enhance cytokine release, which causes persistent pain by sensitizing nociceptive neurons. In addition, the persistent elevation of neurotransmitters such as CGRP, closely related to the progression of neuropathic pain, also suggests a possible mechanism for the development of chronic, non-inflammatory pain in patients with inflammatory joint disease.²⁴ Therefore, this model could be used to test and develop specific drugs for the treatment of post-inflammatory hyperalgesia, clarify the efficacy difference of the specific drug in different stages of inflammation, and optimize the timing of medication.

In clinical studies of RA patients, there is an imbalance of bone absorption and formation in bone metabolism, which can induce the loss of bone mass and eventually lead to OP occurrence. Bone homeostasis is maintained by a balance between osteoclast-induced bone resorption and osteoblast-induced bone formation. Osteoclasts, which are transformed from osteoclast precursors derived from bone marrow, are the only bone-resorptive cells. Osteoclast precursors are present in the peripheral blood and accumulate in the bone reconstruction unit for osteoclast formation in the presence of multiple cytokines. The OPG/RANKL/RANK signaling pathway and Wnt signaling pathway are the main pathway regulating osteoclastogenesis.²⁵ In RA patients, the increased osteoclast differentiation and activity would skew this balance, resulting in progressive bone loss.²⁶ It was found that the bone density of CIA model rats was reduced and trabecular bone structure destroyed,¹⁴ which is consistent with the pathological features of RA with secondary OP. With a prolonged duration of RA or elevated disease activity, osteoclast-related markers were significantly increased²⁷ and maximum load changed in bone biomechanical compression and stretching.

Of course, this research has some limitations. The study only observed the CIA model rats for 4 weeks, which could be used to conduct short-term related studies on pain and OP of RA. It is not clear whether pain and OP could be maintained in the later stage of inflammation in this model. It is impossible to study the pathological mechanism of continuous hyperalgesia after inflammation and to clarify the long-term efficacy of new drug development. Under the conditions with reduced inflammatory injury, further explorations were needed for the study of chronic neuropathic pain and OP.

Conclusion

In this study, we observed the changes in inflammation of CIA model rats and the association with pain and osteoporosis. The results suggest that persistent inflammatory stimuli may lead to the occurrence of central hyperalgesia or neuropathic pain, which suggests that different strategies may be selected for the treatment of pain. Therefore, the anti-inflammatory treatment is preferred to pain symptoms in the early treatment of RA, and the anti-neuropathic pain drugs should be administration in the later stage of the disease. Moreover, the CIA model rats consistently showed bone destruction, suggesting that intervention therapy for bone destruction should be initiated immediately after diagnosis.

Data Sharing Statement

The datasets generated or analyzed in this study are available from the corresponding authors upon reasonable request.

Ethics Approved and Consent to Participate

This study was approved by the Experimental Animal Ethics Committee of Shanxi University and Chinese Medicine (No: 2021DW214). All laboratory operations on Animals follow the Guidelines for the Care and Use of Laboratory Animals published by the National Research Council and published by the National Institutes of Health.

Acknowledgments

This work was financially supported by basic research program in Shanxi province (Grant No.202203021222277); Science and technology innovation project for university in Shanxi Province (Grant No.2022L358); Shanxi Provincial Key Laboratory of classical prescription strengthening yang (Grant No. 202104010910011); scientific research project of Shanxi Provincial Administration of Traditional Chinese Medicine (Grant No.2022ZYYC269); doctoral scientific research fund project (Grant No. 2023BK16, 2023BKS19); key laboratory of rheumatological and immunological diseases treated by integrated Chinese and Western medicine (zyyyjs2024021); 2023 Graduate Innovation and Entrepreneurship Project of Shanxi University of Traditional Chinese Medicine (2023CX027).

Author Contributions

All authors made a significant contribution to the work, whether in its conception, study design, execution, acquisition of data, analysis, and interpretation, or all areas: participated in drafting, revising, or critically reviewing the articles; gave final approval of the version to be published; agreed on the journal for article submission; and agreed to be accountable for all aspects of the work.

Disclosure

The authors declare no conflicts of interest.

References

1. American College of Rheumatology Pain Management Task Force. Report of the American College of rheumatology pain management task force. *Arthritis Care Res.* 2010;62(5):590–599. doi:10.1002/acr.20005
2. Guler MA, Celik OF, Ayhan FF. The important role of central sensitization in chronic musculoskeletal pain seen in different rheumatic diseases. *Clin Rheumatol.* 2020;39(1):269–274. doi:10.1007/s10067-019-04749-1
3. Sarzi-Puttini P, Zen M, Arru F, Giorgi V, Choy EA. Residual pain in rheumatoid arthritis: is it a real problem? *Autoimmun Rev.* 2023;22(11):103423. doi:10.1016/j.autrev.2023.103423
4. Gonçalves WA, Rezende BM, de Oliveira MPE, et al. Sensory ganglia-specific TNF expression is associated with persistent nociception after resolution of inflammation. *Front Immunol.* 2020;10:3120. doi:10.3389/fimmu.2019.03120
5. Liu Y, Caterina MJ, Qu L. Sensory neuron expressed fcγr1 mediates postinflammatory arthritis pain in female mice. *Front Immunol.* 2022;13:889286. doi:10.3389/fimmu.2022.889286
6. He ZH, Zou JT, Chen X, et al. Ångström-scale silver particles ameliorate collagen-induced and K/BxN-transfer arthritis in mice via the suppression of inflammation and osteoclastogenesis. *Inflamm Res.* 2023;72(10–11):2053–2072. doi:10.1007/s00011-023-01778-0
7. Arzamendi MJ, Habibyan YB, Defaye M, et al. Sex-specific post-inflammatory dysbiosis mediates chronic visceral pain in colitis. *Gut Microbes.* 2024;16(1):2409207. doi:10.1080/19490976.2024.2409207
8. Jain A, Hakim S, Woolf CJ. Immune drivers of physiological and pathological pain. *J Exp Med.* 2024;221(5):e20221687. doi:10.1084/jem.20221687
9. Liu X, Huang M, Wang L, Yang C, Zhang M, Wang Q. Decipher the pharmacological mechanisms of raw and wine-processed *Curculigo orchoides* Gaertn. on bone destruction in rheumatoid arthritis rats using metabolomics. *J Ethnopharmacol.* 2023;310:116395. doi:10.1016/j.jep.2023.116395

10. Yang YJ, Lu LJ, Wang JJ, et al. Tubson-2 decoction ameliorates rheumatoid arthritis complicated with osteoporosis in CIA rats involving isochlorogenic acid A regulating IL-17/MAPK pathway. *Phytomedicine*. 2023;116:154875. doi:10.1016/j.phymed.2023.154875
11. Haugeberg G, Uhlig T, Falch JA, Halse JI, Kvien TK. Bone mineral density and frequency of osteoporosis in female patients with rheumatoid arthritis: results from 394 patients in the Oslo county rheumatoid arthritis register. *Arthritis Rheum*. 2000;43(3):522–530. doi:10.1002/1529-0131(200003)43:3<522::AID-ANR7>3.0.CO;2-Y
12. Tengstrand B, Hafström I. Bone mineral density in men with rheumatoid arthritis is associated with erosive disease and sulfasalazine treatment but not with sex hormones. *J Rheumatol*. 2002;29(11):2299–2305.
13. Jin S, Hsieh E, Peng L, et al. Incidence of fractures among patients with rheumatoid arthritis: a systematic review and meta-analysis. *Osteoporos Int*. 2018;29(6):1263–1275. doi:10.1007/s00198-018-4473-1
14. Poutoglidou F, Pourzitaki C, Manthou ME, et al. Infliximab prevents systemic bone loss and suppresses tendon inflammation in a collagen-induced arthritis rat model. *Inflammopharmacology*. 2021;29(3):661–672. doi:10.1007/s10787-021-00815-w
15. Xu R, Peng J, Ma Z, et al. Prolonged administration of total glucosides of paeony improves intestinal immune imbalance and epithelial barrier damage in collagen-induced arthritis rats based on metabolomics-network pharmacology integrated analysis. *Front Pharmacol*. 2023;14:1187797. doi:10.3389/fphar.2023.1187797
16. Liu X, Liu X, Wang H, et al. Quantitative proteomic analysis of circulating exosomes reveals the mechanism by which Triptolide protects against collagen-induced arthritis. *Immun Inflamm Dis*. 2024;12(6):e1322. doi:10.1002/iid3.1322
17. He R, Wang S, Yang S, et al. Shaoyao-Gancao-Tang regulates the T-helper-type 1/T-helper-type 2 ratio in the lung and gut and alters gut microbiota in rats with ovalbumin-induced asthma. *J Ethnopharmacol*. 2023;309:116300. doi:10.1016/j.jep.2023.116300
18. Yeung SC, Ganesan K, Wong SSC, Chung SK, Cheung CW. Characterization of acute pain-induced behavioral passivity in mice: insights from statistical modeling. *Eur J Neurosci*. 2021;53(9):3072–3092. doi:10.1111/ejn.15174
19. Fang W, Huang XH, Qu B, Yang HS. Effect of differences in vertebral cortical bone reinforcement on biomechanics of osteoporotic vertebral compression fractures[J/OL]. *Chin J Tissue Eng Res*. 2024;1–9.
20. Scholz J, Finnerup NB, Attal N, et al. Classification Committee of the Neuropathic Pain Special Interest Group (NeuPSIG). The IASP classification of chronic pain for ICD-11: chronic neuropathic pain. *Pain*. 2019;160(1):53–59. doi:10.1097/j.pain.0000000000001365
21. Cao Y, Fan D, Yin Y. Pain mechanism in rheumatoid arthritis: from cytokines to central sensitization. *Mediators Inflamm*. 2020;2020:2076328. doi:10.1155/2020/2076328
22. Ten Klooster PM, de Graaf N, Vonkeman HE. Association between pain phenotype and disease activity in rheumatoid arthritis patients: a non-interventional, longitudinal cohort study. *Arthritis Res Ther*. 2019;21(1):257. doi:10.1186/s13075-019-2042-4
23. Nieto FR, Clark AK, Grist J, Chapman V, Malcangio M. Calcitonin gene-related peptide-expressing sensory neurons and spinal microglial reactivity contribute to pain states in collagen-induced arthritis. *Arthritis Rheumatol*. 2015;67(6):1668–1677. doi:10.1002/art.39082
24. Zhang A, Lee YC. Mechanisms for joint pain in Rheumatoid Arthritis (RA): from cytokines to central sensitization. *Curr Osteoporos Rep*. 2018;16(5):603–610. doi:10.1007/s11914-018-0473-5
25. Li X, Chen W, Liu D, et al. Pathological progression of osteoarthritis: a perspective on subchondral bone. *Front Med*. 2024;18(2):237–257. doi:10.1007/s11684-024-1061-y
26. Li YN, Chen CW, Trinh-Minh T, et al. Dynamic changes in O-GlcNAcylation regulate osteoclast differentiation and bone loss via nucleoporin 153. *Bone Res*. 2022;10(1):51. doi:10.1038/s41413-022-00218-9
27. Komatsu N, H T. Mechanisms of joint destruction in rheumatoid arthritis - immune cell-fibroblast-bone interactions. *Nat Rev Rheumatol*. 2022;18(7):415–429. doi:10.1038/s41584-022-00793-5

Publish your work in this journal

The Journal of Inflammation Research is an international, peer-reviewed open-access journal that welcomes laboratory and clinical findings on the molecular basis, cell biology and pharmacology of inflammation including original research, reviews, symposium reports, hypothesis formation and commentaries on: acute/chronic inflammation; mediators of inflammation; cellular processes; molecular mechanisms; pharmacology and novel anti-inflammatory drugs; clinical conditions involving inflammation. The manuscript management system is completely online and includes a very quick and fair peer-review system. Visit <http://www.dovepress.com/testimonials.php> to read real quotes from published authors.

Submit your manuscript here: <https://www.dovepress.com/journal-of-inflammation-research-journal>